Supplementary material

Evaluation of Surface Properties in Biosilica-Reinforced Bi-obased Polyester Nanocomposites

Hifa Salah Adeen Embirsh[1], Ivana O. Mladenović[2], Vesna Radojević[1], Aleksandar Marinković[1], Marija M. Vuksanović[3,*]

[1]*University of Belgrade, Faculty of Technology and Metallurgy, 11120 Belgrade, Serbia; yhaifa23@yahoo.com (H.S.A.E.), marinko@tmf.bg.ac.rs (A.M.), vesnar@tmf.bg.ac.rs (V.R.)*

[2]*University of Belgrade, Institute of Chemistry, Technology and Metallurgy - National Institute of the Republic of Serbia, 11000 Belgrade, Serbia; ivana.mladenovic@ihtm.bg.ac.rs (I.O.M.)*

[3]*University of Belgrade, Department of Chemical Dynamics and Permanent Education, „VINČA" Institute of Nuclear Sciences - National Institute of the Republic of Serbia, 11351 Belgrade, Serbia; mari-ja.vuksanovic@vin.bg.ac.rs (M.M.V.)*

Corresponding author: Marija Vuksanović, e-mail: marija.vuksanovic@vin.bg.ac.rs

S1. Materials and Methods

S1.1. Preparation and Modification of Biosilica Particles

S1.1.1. Thermogravimetric Analysis

To assess the differences in thermal stability among the biosilica nanoparticles, thermogravimetric (TG) and derivative thermogravimetric (dTG) analyses were conducted (Figure S1). The unmodified silica demonstrated high thermal stability throughout the entire temperature range, with no detectable surface moisture [64]. SiO_2-M exhibited approximately 1% weight loss between 28 °C and 250 °C, attributed to the evaporation of surface-bound moisture and volatile organic compounds [11]. In the second region, spanning from 250 °C to 550 °C, thermal degradation of the organic modifier occurred, with a dTG peak at 424.9 °C and a corresponding weight loss of 3.5%. The total weight loss for SiO_2-M was 4.5%. For SiO_2-V, about 1% weight loss was observed up to 100 °C, associated with surface moisture. A gradual weight loss continued up to 530 °C, followed by a minor but sharper decrease of 0.5%. The total weight loss for this sample was approximately 2.7%. SiO_2-AMBD showed a more pronounced weight loss of 2.3% up to 90 °C. Between 350 °C and 600 °C, an additional 3.9% weight loss was recorded, with a dTG peak at 427.9 °C. The total weight loss reached 8.05%, indicating the complex structure and thermally sensitive nature of the surface functionalization.

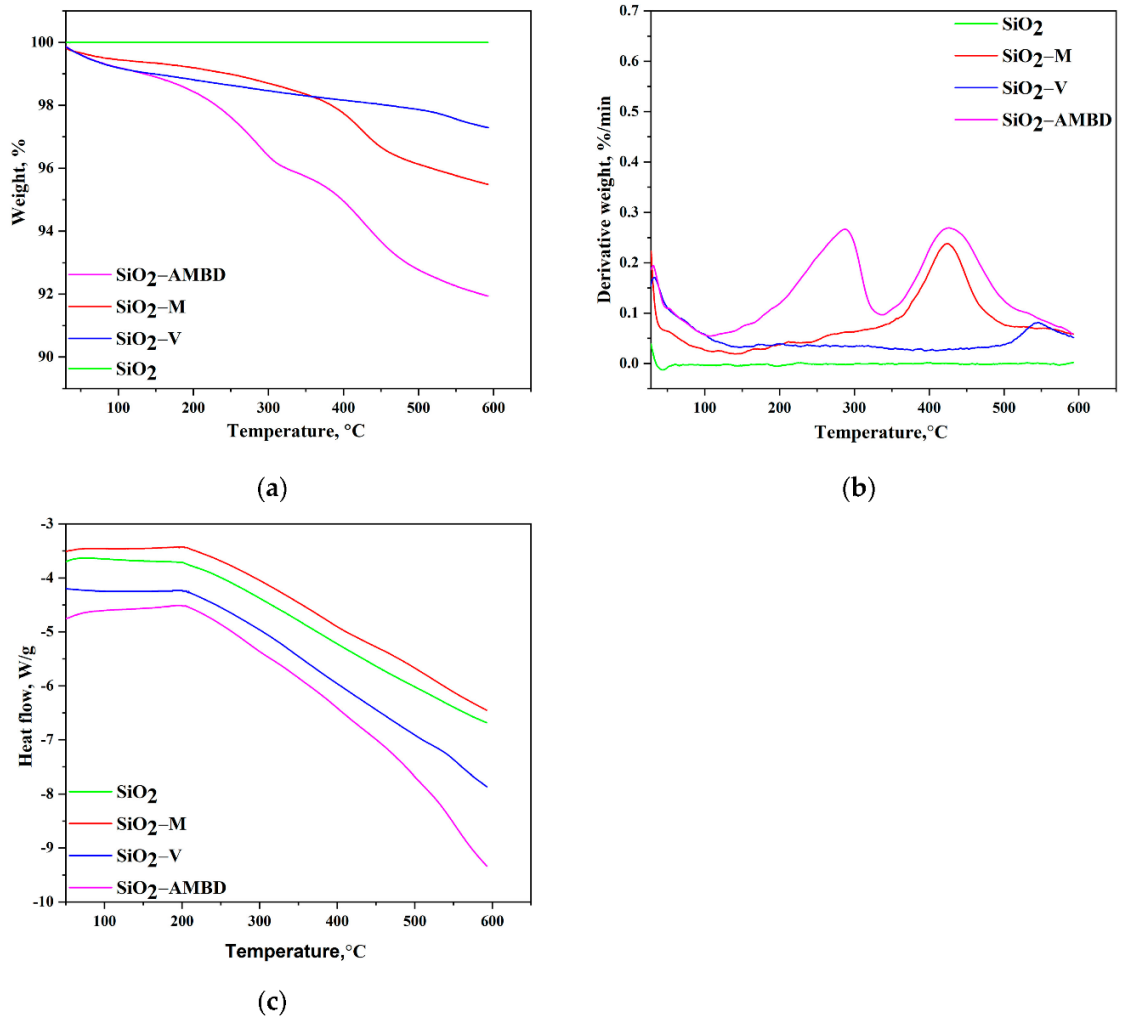


Figure S1. Thermogravimetric analysis of unmodified and modified biosilica particles: (a) TG, (b) dTG, and (c) DSC curves [1]

S1.2. Preparation of b-UPR composites

The results of ^{1}H and ^{13}C NMR and FTIR analyses indisputably confirm the success of the synthesis of UPR resins based on PET/PG glycolysate. The results from structural study of ^{1}H and ^{13}C NMR analysis of synthesized resin are reported below (Figures S2 and S3).

^{1}H NMR ($CDCl_3$, δ/ppm): 1.11–1.38 (3H, m, -CH_3), 3.58-4.71 (14H, m, b-CH_2 and c-CH_2), 5.16-5.35 (1H, m, d-CH), 5.70-5.80 (2H, d, styrene moiety), 6.30-6.84 (4H, m, a-CH=CH), 7.25-7.43 (1H, m, ph-styrene moiety), 8.05-8.12 (12H, m, e-CHph). ^{13}C NMR ($CDCl_3$, δ/ppm): 16.42 (-CH_3), 62.81-67.83 (b-CH_2), 70.37-71.35 (c-CH_2), 73.35-73.75 (d-CH), 113.76 (Cph-styrene moiety) 126.16-129.73 (e-CHph), 132.86-134.52 (a-CH=CH), 136.83 (h-Cph), 164.52 (g-C=O), 165.49 (f-C=O) [1]

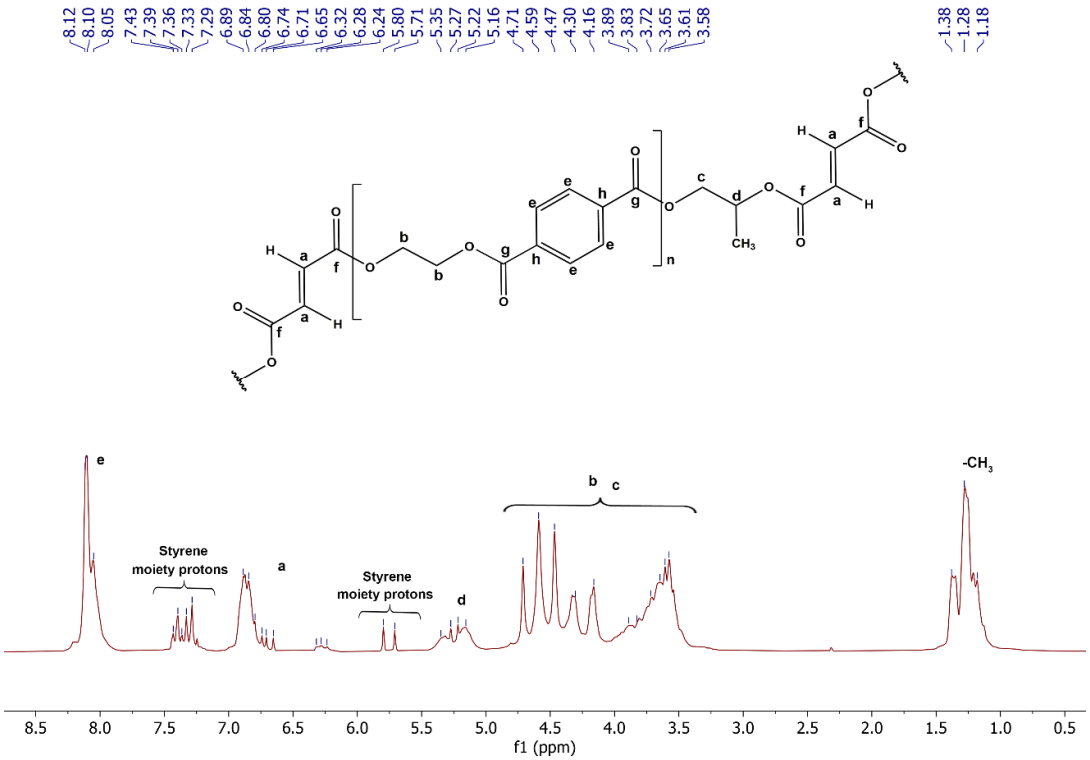


Figure S2. [1]H NMR spectrum of b-UPR resin [1]

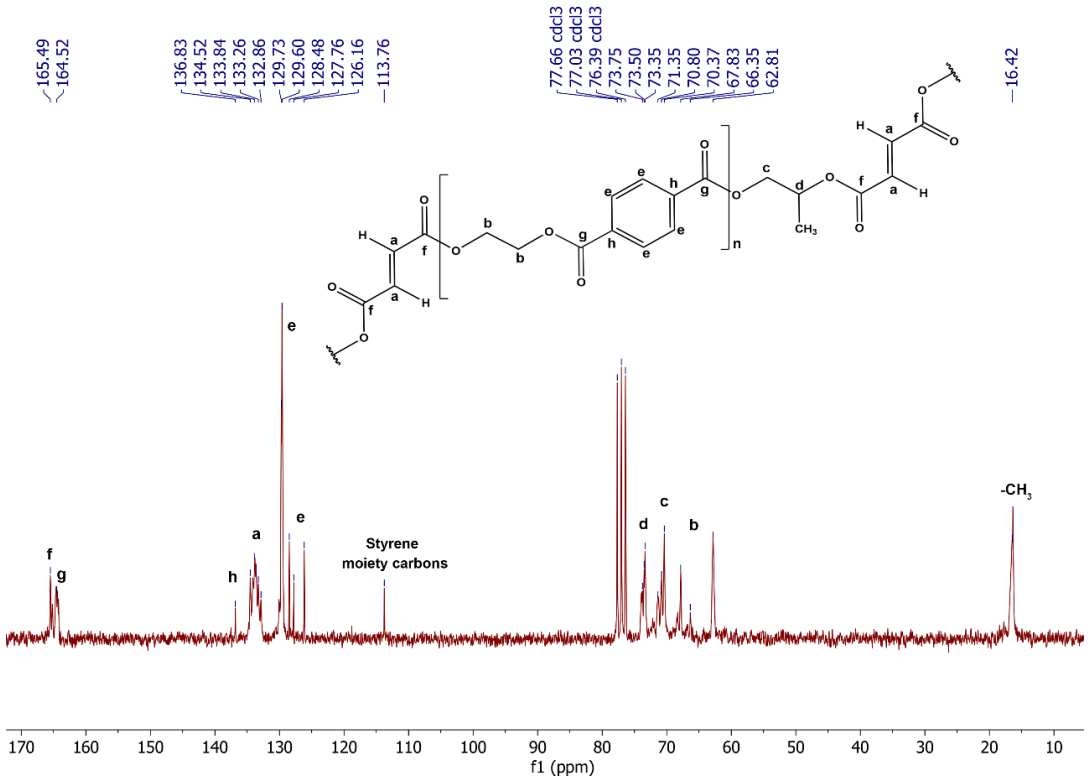


Figure S3. [13]C NMR spectrum of b-UPR resin [1]

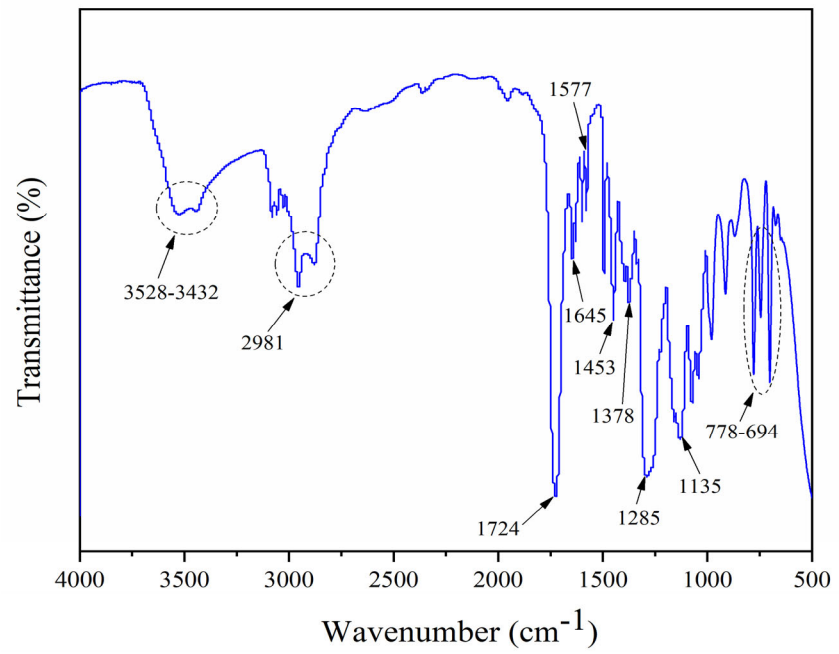


Figure S4. FTIR spectra of b-UPR resin [1]

Figure S3 The FTIR spectra of UPR resins synthesized from the products of catalytic depolymerization of PET more than PG by the classical glycolysis method. The wide band shown at 3432 – 3528 cm^{-1} corresponds to the elongation vibrations of the OH groups from the residual reactants. The band at about 2981 cm^{-1} originates from the vibration of stretching of aliphatic C-H bonds from the methyl and methylene groups. The peak corresponding to the stretching of the C = O group has shifted the maximum absorption vibration to a higher frequency - 1724 cm^{-1}. The changes in intensity observed at 1645 cm^{-1} and 1578 cm^{-1} represent the vibrations of the C = C bonds in the phenyl nucleus. Bending vibrations in the plane of C-H bonds in the CH_3 group, symmetric and asymmetric, are observed at 1378 cm^{-1} and 1453 cm^{-1}, respectively. The peak at 1274 cm^{-1} corresponds to the vibrations of the C-O bond. In the area 778 - 694 cm^{-1}, deformation C-H vibrations outside the plane of aromatic compounds are observed [1].

In the spectra of all biosilica particles (Figure S4a), a broad band observed between 3366 cm^{-1} and 3323 cm^{-1} corresponds to the stretching vibrations of –OH groups [2]. A strong peak at 1046 cm^{-1} is attributed to Si–O–Si network vibrations, along with siloxane stretching vibrations near 797 cm^{-1} [3,4]. The absence of organic bands in SiO_2 indicates the high purity of the biosilica derived from RHS. Symmetric and asymmetric $–CH_2$ stretching vibrations are detected at 2930 and 2859 cm^{-1}, while bending vibrations of these groups appear in the range of 1517–1370 cm^{-1} [5,6]. In the SiO_2-AMBD spectrum, the presence of

the amide I band at 1650 cm^{-1} and N–H bending at 872 cm^{-1} confirm successful functionalization with APTES [7], followed by further modification using soybean oil fatty acid methyl esters.

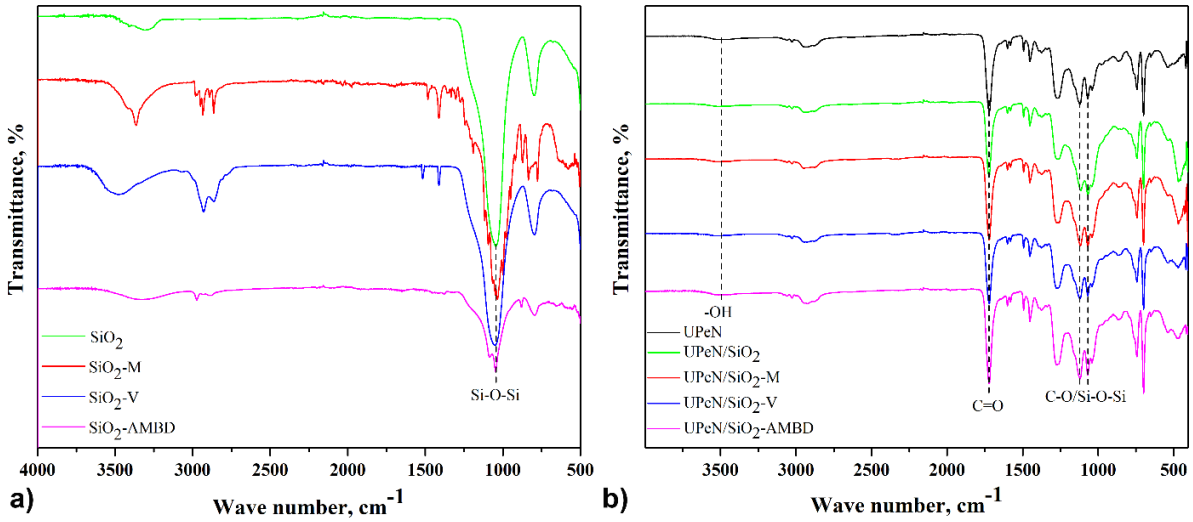


Figure S5. FTIR spectra of (a) biosilica nanoparticles and (b) b-UPR composites [1]

Interfacial interactions between biosilica and b-UPR were analyzed by comparing the spectra of the neat matrix and the nanocomposite containing 5 wt.% of nanoparticles. In all spectra (Figure 4Sb), a weak –OH stretching band is observed around 3493 cm^{-1} [2]. Aromatic C–H stretching appears at 3027 cm^{-1}, while aliphatic C–H stretching vibrations from $–CH_3$ and $–CH_2$ groups are located at 2947 and 2878 cm^{-1}, respectively. The absorption band at 1725 cm^{-1} corresponds to carbonyl (C=O) stretching within the terephthalic acid ester units [8]. Peaks at 1452 and 1371 cm^{-1} are associated with the bending vibrations of CH_3 and CH_2 groups. C–O stretching vibrations are observed at 1268, 1121, and 1066 cm^{-1} [9,10]. In the nanocomposite spectrum, slight shifts from 1121 to 1119 cm^{-1} and from 1066 to 1070 cm^{-1} are detected, likely due to overlapping with Si–O–Si stretching bands. Aromatic –CH bending vibrations of benzene rings appear at 745 and 706 cm^{-1}.

S2. SEM/TEM Analysis of Biosilica Fillers, b-UPR Nanocomposite and AFM Analysis

Field emission scanning electron microscopy (FESEM) was employed to investigate the morphology of unmodified biosilica (Figure S6a) and surface-modified SiO_2-V particles (Figure S6b). The nanostructure of the silica particles remained largely unchanged after modification. To further analyse the dispersion, morphology, and particle size.

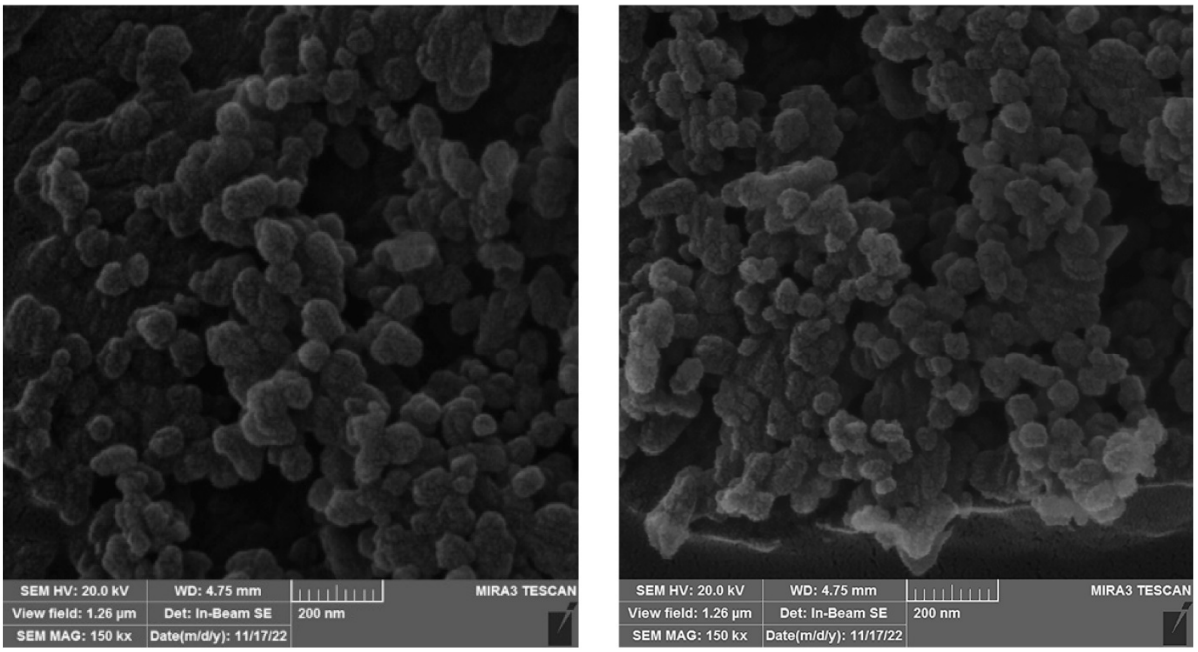
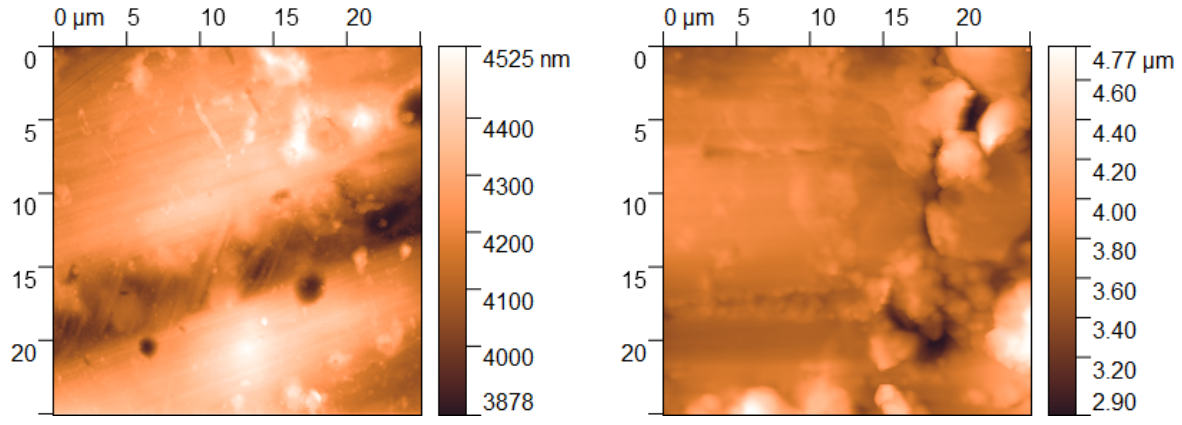


Figure S6. FESEM micrograph of unmodified silica particles: (a) unmodified, and (b) modified SiO_2-V [1]

In the 2D images, AFM can distinguish between spike tips (agglomerates of silica) and holes and valleys (b-UPR matrix or location with air). The hybrid nanocomposites, which are harder and more crystalline than the pristine system, as confirmed by microhardness data, predominantly display hard phases of silica.



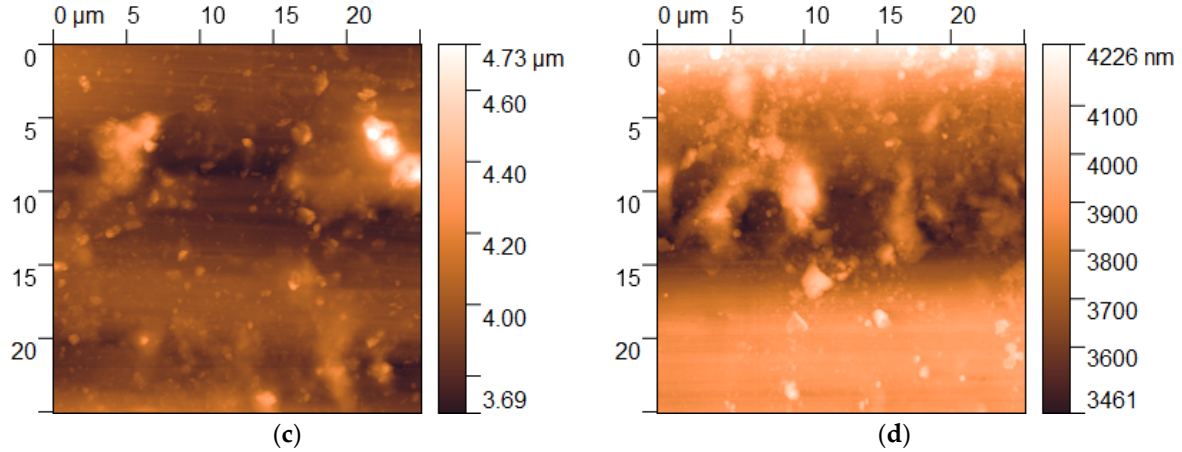


Figure S7. AFM 2D Images of the Nanocomposites Containing 1.0 wt.% Biosilica Nanoparticles: (a) b-UPR/SiO_2, (b) b-UPR/SiO_2-AMBD, (c) b-UPR/SiO_2-M, and (d) b-UPR/SiO_2-V.

Figure S8 presents FESEM images of the fractured surfaces of polyester composites reinforced with 2.5 wt.% of both unmodified and surface-modified biosilica.

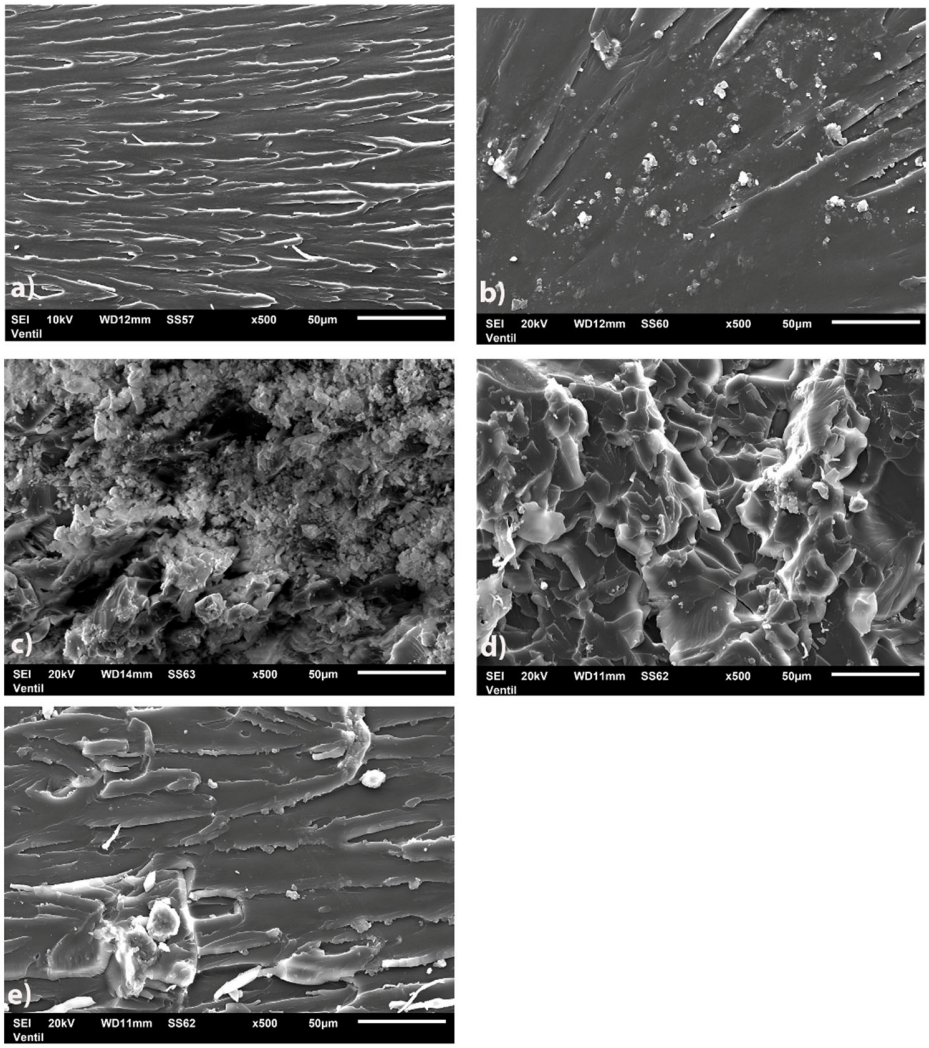


Figure S8. FESEM images of (a) polyester samples as well as nanocomposite with 2.5 wt.% of biosilica nanoparticles (b) b-UPR/SiO_2, (c) b-UPR/SiO_2-V, (d) b-UPR/SiO_2-AMBD and (e) b-UPR/SiO_2-M [1]

References

1. Embirsh, H.S.A.; Stajčić, I.; Gržetić, J.; Mladenović, I.O.; Anđelković, B.; Marinković, A.; Vuksanović, M.M. Synthesis, Characterization and Application of Biobased Unsaturated Polyester Resin Reinforced with Unmodified/Modified Biosilica Nanoparticles. *Polymers (Basel).* **2023**, *15*, 3756, doi:10.3390/polym15183756.
2. Radovic, I.; Stajcic, A.; Radisavljevic, A.; Veljkovic, F.; Cebela, M.; Mitic, V. V.; Radojevic, V. Solvent Effects on Structural Changes in Self-Healing Epoxy Composites. *Mater. Chem. Phys.* **2020**, *256*, 123761, doi:10.1016/j.matchemphys.2020.123761.
3. Zou, H.; Wu, S.; Shen, J. Polymer/Silica Nanocomposites: Preparation, Characterization, Properties, and Applications. *Chem. Rev.* **2008**, *108*, 3893–3957, doi:10.1021/cr068035q.
4. Azat, S.; Korobeinyk, A.V.; Moustakas, K.; Inglezakis, V.J. Sustainable Production of Pure Silica from Rice Husk Waste in Kazakhstan. *J. Clean. Prod.* **2019**, *217*, 352–359, doi:10.1016/j.jclepro.2019.01.142.
5. Lee, H.; Abarghani, A.; Liu, B.; Shokouhimehr, M.; Ostadhassan, M. Molecular Weight Variations of Kerogen during Maturation with MALDI-TOF-MS. *Fuel* **2020**, *269*, 117452, doi:10.1016/j.fuel.2020.117452.
6. Janković, B.; Manić, N.; Radović, I.; Janković, M.; Rajačić, M. Model-Free and Model-Based Kinetics of the Combustion Process of Low Rank Coals with High Ash Contents Using TGA-DTG-DTA-MS and FTIR Techniques. *Thermochim. Acta* **2019**, *679*, 178337, doi:10.1016/j.tca.2019.178337.
7. Rusmirovic, J.D.; Trifkovic, K.T.; Bugarski, B.; Pavlovic, V.B.; Dzunuzovic, J.; Tomic, M.; Marinkovic, A.D. High Performances Unsaturated Polyester Based Nanocomposites: Effect of Vinyl Modified Nanosilica on Mechanical Properties. *Express Polym. Lett.* **2016**, *10*, 139–159, doi:10.3144/expresspolymlett.2016.14.
8. Lazouzi, G.A.; Vuksanović, M.M.; Tomić, N.; Petrović, M.; Spasojević, P.; Radojević, V.; Jančić Heinemann, R. Dimethyl Itaconate Modified PMMA - Alumina Fillers Composites With Improved Mechanical Properties. *Polym. Compos.* **2019**, *40*, doi:10.1002/pc.24952.
9. Spasojević, P.M.; Panić, V. V.; Džunuzović, J. V.; Marinković, A.D.; Woortman, A.J.J.; Loos, K.; Popović, I.G. High Performance Alkyd Resins Synthesized from Postconsumer PET Bottles. *RSC Adv.* **2015**, *5*, 62273–62283, doi:10.1039/C5RA11777A.
10. Kirshanov, K.; Toms, R.; Melnikov, P.; Gervald, A. Unsaturated Polyester Resin Nanocomposites Based on Post-Consumer Polyethylene Terephthalate. *Polymers (Basel).* **2022**, *14*, 1602,

doi:10.3390/polym14081602.

11. Rusmirović, J.D.; Ivanović, J.Z.; Pavlović, V.B.; Rakić, V.M.; Rančić, M.P.; Djokić, V.; Marinković, A.D. Novel Modified Nanocellulose Applicable as Reinforcement in High-Performance Nanocomposites. *Carbohydr. Polym.* **2017**, *164*, 64–74, doi:10.1016/j.carbpol.2017.01.086.